13th International Conference on
Structural Health Monitoring of Intelligent Infrastructure
DOI: 10.3217/978-3-99161-057-1-022

Structural performance monitoring for concrete girder bridges with distributed fiber optic sensors

Francesco Fabbricatore[1, ORCID (0009-0003-2198-6868)], Numa Bertola[2, ORCID (0000-0002-4151-3123)]
[1] Department of Engineering, Faculty of Science, Technology and Medicine, University of Luxembourg, Maison du Nombre 6, Avenue de la Fonte, L-4364 Esch-Sur-Alzette, Luxembourg.
email: francesco.fabbricatore@uni.lu, numa.bertola@unil.lu

ABSTRACT: The alarming frequency of bridge collapses in recent years underscores the critical need for advanced monitoring strategies tailored to existing infrastructure. Many concrete bridges, built decades ago, now face increasing traffic demands and environmental stressors that threaten their structural integrity.
This study investigates the use of distributed fiber optic sensors (DFOSs) with high spatial resolution (independent strain measurements every 2.6 mm) during static load tests to assess the structural performance of concrete girder bridges. The goal is to gain a deeper understanding of their condition using data-driven approaches. The fiber optic technology provides detailed strain profile information that gives insights into global bridge behavior, such as stress distributions, support conditions and static responses. It also allows the detection of cracks along the fiber path and other localized effects that may remain undetected without a calibrated numerical model.
This method of structural performance monitoring is applied to a prestressed concrete bridge in Switzerland. Static load tests have been performed on a full-scale bridge in Switzerland and the resulting distributed strain datasets allow the accurate understanding of bridge behavior, including deflection extrapolation and crack detection. The results underline the potential of DFOS to develop novel data-driven solutions for extending the service life of structures.

KEY WORDS: Distributed fiber optic sensors, Structural identification, Structural performance monitoring, Structural health monitoring, Load testing, Concrete bridge.

1 INTRODUCTION

Across the globe, bridge networks are experiencing a rapid deterioration amid rising traffic demands and environmental effects, posing significant challenges to infrastructure safety and management. Budgetary constraints and the potential socioeconomic disruptions from closures or failures, such as the catastrophic collapse of the Morandi Bridge in Genoa [Calvi et al., 2019], highlight the critical need for accurate structural safety assessments to optimize resource allocation and ensure public safety.
Traditional engineering approaches, created for the design of new structures, are not adapted to existing bridges, where material degradation and unforeseen modifications obscure true conditions. Compounding this issue, visual inspections suffer from subjectivity and an inability to detect hidden flaws, driving the need for more reliable, data-driven solutions [1]. To address these shortcomings, researchers have developed advanced monitoring methodologies that harness field measurements to either pinpoint damage or deepen understanding of structural behavior [2]. Structural performance monitoring (SPM), in particular, seeks to uncover hidden reserves of load-bearing capacity by leveraging precise measurements from real-world conditions [3]. The effectiveness of such frameworks hinges on the choice of monitoring technology. Since the 1950s, strain gauges have been a cornerstone of structural assessment, valued for their affordability and durability [4]. However, their discrete spatial sampling limits their ability to capture the full spectrum of a bridge response, especially in aging concrete structures prone to localized deterioration.

The introduction of fiber optic sensors (FOS) has marked a pivotal advancement, enabling distributed strain monitoring over extended distances with high spatial resolution [5]. More recently, distributed fiber optic sensors (DFOS) have pushed this boundary further, achieving gauge pitches as fine as 1.3–2.6 mm through breakthroughs in optical technology. This development, depicted in Figure 1, facilitates precise detection of local strain anomalies, such as impacts of concrete cracks, by analyzing time- and frequency-domain signals, far exceeding the capabilities of traditional sensors [6].

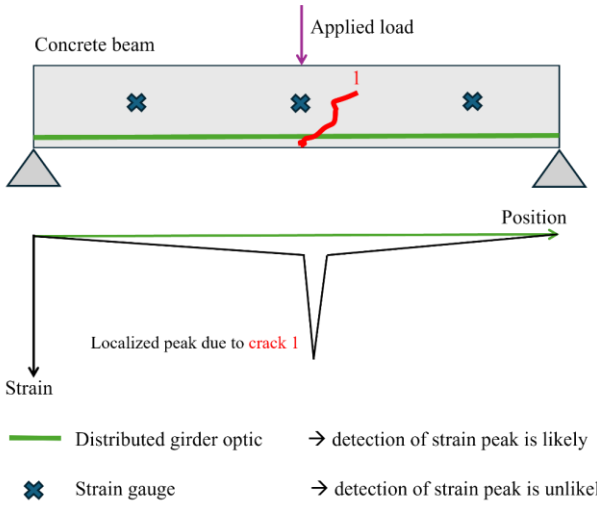

Figure 1. Comparison between distributed fiber optic sensors and conventional strain gauge for concrete-structure monitoring.

DOI: 10.3217/978-3-99161-057-1-022

Despite these advances, notable gaps remain in the literature. Most research focuses on long-term structural health monitoring (SHM) to track trends over time [7], while the potential of DFOS for SPM, evaluating immediate responses under specific loads, remains largely untapped.

This study explores the transformative potential of DFOS in concrete bridge monitoring, with a focus on the role of signal processing in unlocking comprehensive structural understanding. Using datasets collected during static load tests on a full-scale prestressed concrete bridge, the approach demonstrates how DFOS-derived strain profiles provide a dual lens, detecting local effects like cracks and elucidating global responses like girder interactions and boundary effects. The primary objective of this study is to show the result of application a novel SPM methodology that integrates DFOS technology with static load testing to provide detailed evaluations of both local and global structural behaviors [8].

This approach is applied to an existing prestressed concrete bridge, Ferpècle bridge in Switzerland. This methodology illustrates the substantial benefits of DFOS and signal processing in providing a holistic understanding in enhancing safety, optimizing maintenance strategies, and extending the service life of critical infrastructure.

2 BRIDGE BEHAVIOURS IDENTIFICATION – 6 STEPS METHODOLOGY

Evaluating the structural integrity of existing bridges, especially those with complex geometries, demands detailed knowledge of their characteristics and construction history, yet such information is frequently incomplete or absent for older structures. This section outlines a new methodology [8] that utilizes static load test data to generate new insights, enhancing the accuracy of structural assessments. The methodology, illustrated in Figure 2, centers on SPM of girder bridges using DFOS.

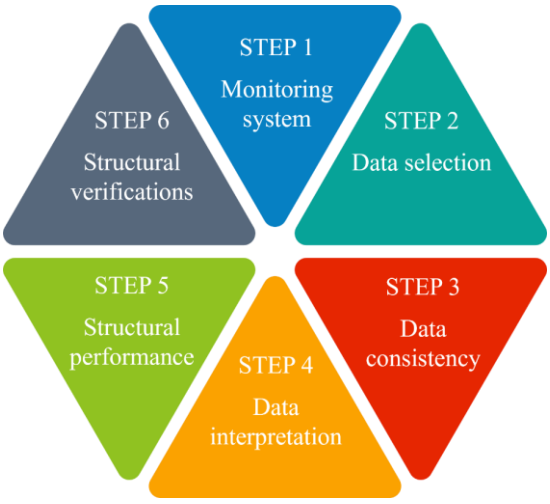

Figure 2. Overview of the methodology for the examination of existing girder concrete bridges with DFOS.

Step 1 involves selecting monitoring systems and load test configurations to acquire informative datasets. Multiple DFOS, coupled with a high-resolution data acquisition system, capture strain responses with fine spatial detail during controlled static load tests. Supplementary sensors, such as linear variable differential transformers (LVDTs), may be incorporated to augment data richness. Step 2 entails analyzing and refining the collected data. At each measurement point, the most probable value is extracted and anomalies are filtered to ensure only reliable, representative data proceed to analysis. In Step 3, the consistency of strain data is validated against expected values derived from the bridge structural properties and the load test configurations. Step 4 examines the strain distribution to determine the bridge's static behavior, revealing global structural patterns and localized effects, such as concrete cracks (via strain peaks) and the impact of secondary elements on main girder deformations.

Step 5 extrapolates stress distributions among girders, support conditions, and bridge deflection from the strain data, yielding refined insights into structural behavior for improved assessments. Step 6 addresses structural safety through standard verifications, though these lie beyond this study's scope; further details are available in [9]. This model-free approach systematically converts raw data into actionable knowledge, facilitating a comprehensive understanding of three-dimensional bridge behavior.

3 STRUCTURAL PERFORMANCE MONITORING WITH DISTRIBUTED FIBER OPTIC SENSORS

3.1 Bridge presentation

Located in Les Haudères in the Swiss Alps (canton of Wallis) at an altitude of 1450 meters, the Ferpècle Bridge is a prestressed reinforced concrete structure erected in 1958. Designed with a single 35-meter span, the bridge originally consisted of two girders, each 1.5 meters high, arranged in a slender TT cross-section and is one of the first prestressed bridges in the country (Figure 3). In 2023, a structural intervention expanded the deck width from 5.3 meters to 7.9 meters using ultra-high-performance fiber-reinforced cementitious composite (UHPFRC). This intervention employed a cantilevered UHPFRC slab with varying thickness, rigidly linking the superstructure to the abutments and converting the bridge into a semi-integral static system (Figure 4) [9].

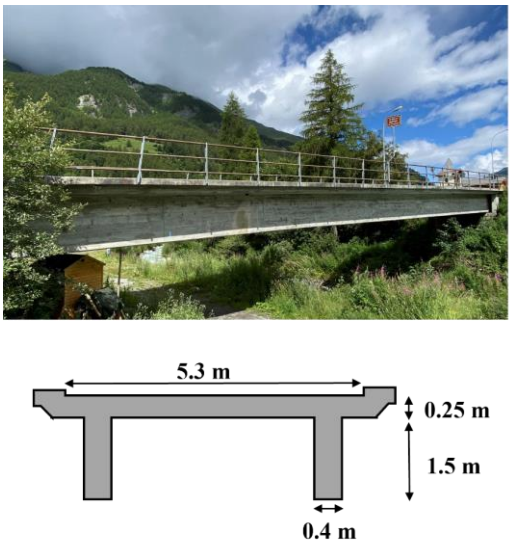

Figure 3. Photograph and cross-section scheme before intervention.

DOI: 10.3217/978-3-99161-057-1-022

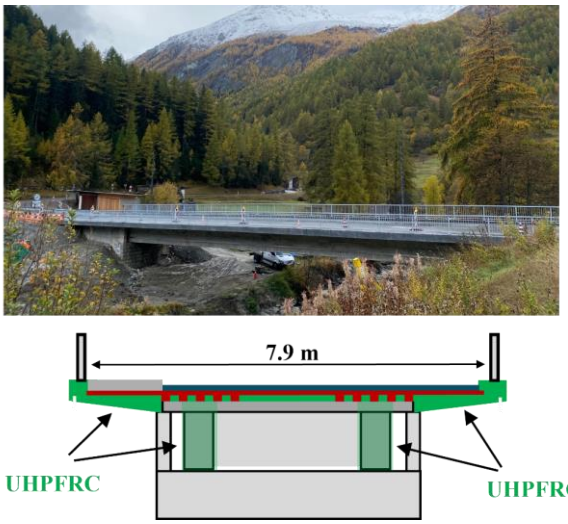

Figure 4. Photograph and cross section scheme after intervention.

This structural modification, accomplished by establishing a monolithic connection between the superstructure and abutments, redistributes bending moments, removes expansion joints and increases support capacity. As a result, the bridge benefits from significantly enhanced rigidity, bending capacity, and shear strength, while the low permeability of UHPFRC improves its long-term durability.

Materially, the bridge was initially built with C30/37 concrete, now reassessed as C40/50 to account for strength increases over time [10]. The reinforcing steel has a characteristic tensile yield stress of f_{yk}=345 MPa, and the prestressed bars feature a strength of f_{pd}=840 MPa. The UHPFRC, categorized as type UB, meets Swiss standards with a tensile strength of f_{Utud}=6.9 MPa [11].

3.2 Distributed fiber optic monitoring campaign

Comprehensive monitoring campaigns were conducted in 2023 and 2024, following the intervention on the Ferpècle Bridge to evaluate its structural behavior and mechanical properties. During the deck widening from 5.3 to 7.9 meters, scaffolding facilitated the installation of distributed fiber optic sensors (DFOS) along the full 35-meter span of both prestressed concrete girders. Grooves 6 mm deep were cut into the external web of each girder, 0.5 meters from the girder bottom. DFOS cables (SMARTEC-DiTeSt SMARTProfile Sensor [12]) were affixed with glue and protected by aluminum plates to shield against environmental exposure, as illustrated in Figure 5. This figure also depicts the fiber optic positioning process and a schematization of the SMARTEC sensor, which incorporates two fibers for detecting temperature variations and two for measuring strain, both monolithic sensors with standard acrylate coating, further shielded by UHPFRC cantilevers. The installation presented challenges, requiring a scaffolding to groove the concrete and the careful gluing of fiber optic cables to avoid sensor slip. Uniform glue distribution was critical to ensure consistent response in the concrete-glue-coating-sensor system. The upstream girder is designated Channel 1 (CH1) and the downstream girder Channel 2 (CH2). Strain data were recorded using a LUNA ODiSI 6100 system [13] at a 2.6 mm resolution, yielding approximately 12,000 data points per girder, at a 5 Hz sampling rate. Five static load tests were performed using one or two three-axle trucks, each weighing 26.4 tons (axle loads: 8.9 tons, 10.4 tons, 7.1 tons; transverse axle spacing: 2.0 meters). These configurations, detailed in Figure 4, included single-truck midspan loading (LT1 and LT2), dual-truck side-by-side placement at midspan (LT5) and longitudinal alignment along one girder (LT1 and LT2) to maximize the effects in one-quarter span.

Figure 5: SMARTEC fiber optic installation

Six linear variable differential transformers (LVDTs) were installed vertically beneath the girders at midspan, near abutments and quarter-span positions, recording deflection at 10 Hz to complement DFOS datasets.

A similar monitoring campaign was conducted in 2024, differing only in the repositioning of the two LVDTs from near the abutments to the transverse beam at quarter-span locations and an increase in truck load to approximately 28 tons.

For both campaigns, temperature compensation was deemed unnecessary due to the short data collection period (approximately 30 minutes) and cloudy sky conditions. These conditions did not result in temperature changes significant enough to alter the structural response compared to the calibration baseline. This assumption is validated by the strain and LVDT signals in the time domain, as shown in Figure 9, where signals start at zero when no truck is on the bridge and return to zero after the truck leaves, indicating no effects necessitating temperature compensation.

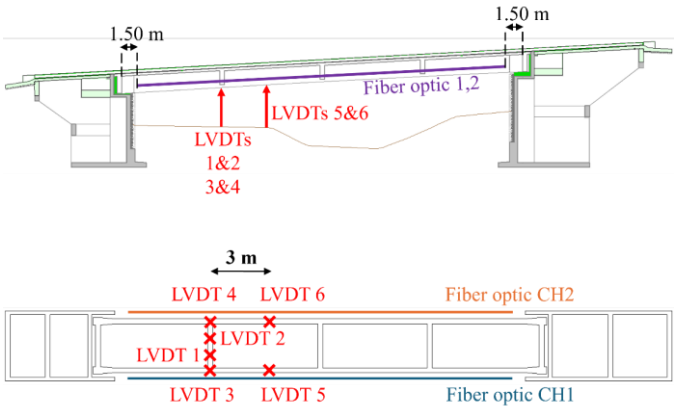

Figure 6. Sensor configuration. (Up) Elevation view; (Down) Plan view.

DOI: 10.3217/978-3-99161-057-1-022

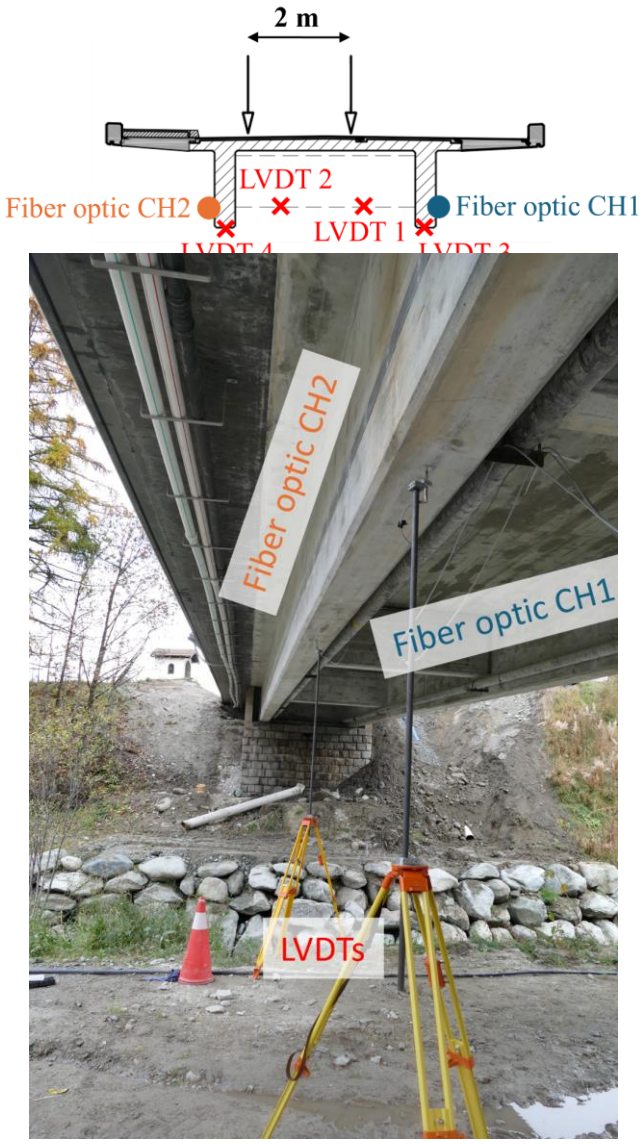

Figure 7. Sensor configuration. (Up) Cross section in one quarter-span for the load configuration LT3; (Down) Photo of the bridge with sensor locations.

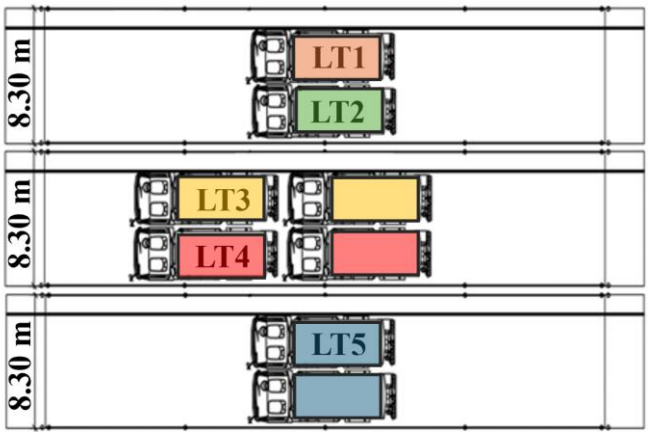

Figure 8. Static load tests with either one truck (LT1 and LT2) or two trucks (LT3, LT4 and LT5).

Each test produced two strain vectors per girder (N × T dimensions, where N ≈ 12,000 points and T denotes time steps), totaling ten vectors across the campaign. LVDTs yielded six deflection vectors per test (1 × T dimensions), totaling 30 vectors.

3.3 Application of the methodology for LT3

The methodology of Section 2 is applied considering the strain measurements by the DFOS for CH2 during LT3 from the monitoring campaign of 2024.

As a first step, the raw DFOS and LVDT data are processed to extract reliable structural response measurements. Consistent strain and deflection values are determined by averaging measurements taken while the trucks remain stationary (Figure 9), filtering out anomalies. For CH2, the most probable strain value at a midspan DFOS point is 20 με while for LVDT4 (one quarter span of CH2), the deflection is 2.32 mm. Post-selection, DFOS datasets are reduced from N × T to N × 1 vectors (N ≈ 12,000), and LVDT datasets from 1 × T to 1 × 1, streamlining subsequent analysis. Figure 10 illustrates the reconstructed signal for LT3 in CH2.

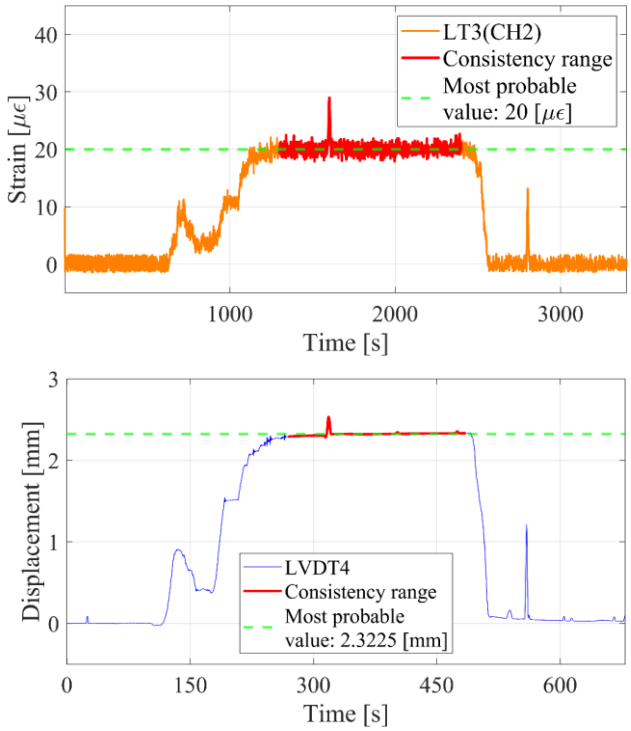

Figure 9. Signal selection. (Up) Strain value at a specific DFOS measurement of CH2 under LT3; (Down) Deflection value for LVDT4 under LT3.

The reliability of LT3 strain data is validated by confirming their consistency with expected structural behavior. The strain distribution for LT3, as shown in Figure 10, aligns fully with the load configuration and the fixed-fixed static scheme. Strain data exhibit negative values near the abutments, positive values at midspan, and zero values near the transverse beams at the one-quarter and three-quarter span positions, following the expected bending-moment diagram. Notably, the strain on the left side of the diagram is higher at the one-quarter span than at

DOI: 10.3217/978-3-99161-057-1-022

the three-quarter span, which is entirely consistent since the load is applied at the one-quarter span.

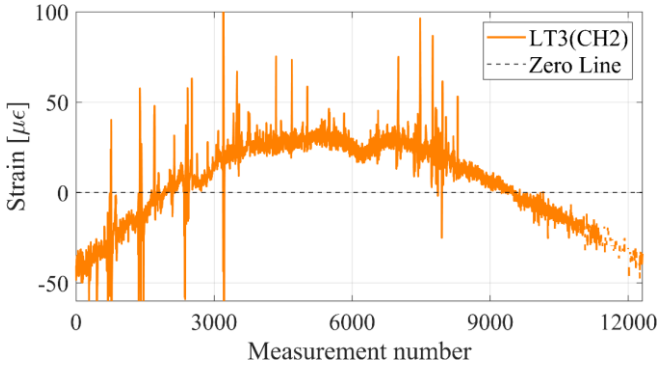

Figure 10. Reconstructed strain signal with the selected value at every DFOS measurement location of CH2 under LT3.

Beyond the noise range (approximately ± 5 με), strain peaks are observed on the left side and near midspan on the right side, represented by red dots in Figure 11.

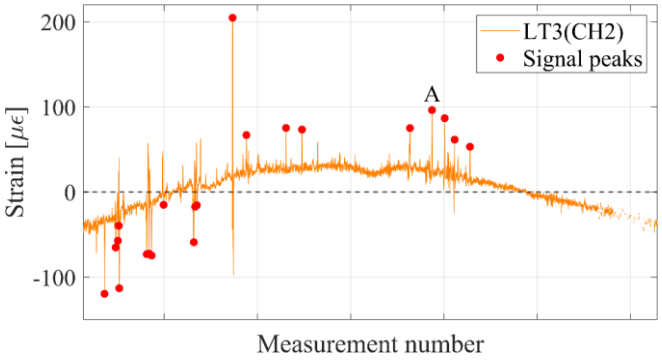

Figure 11. Peaks characterization for LT3 data in CH2.

These peaks are localized using the prominence technique [14], which identifies significant strain values by measuring how much they stand out from their surroundings. The strain peaks are detected in the negative strain zone when the strain is negative (at the initial and end sides of the bridge) and in the positive strain zone when the strain is positive (at the middle of the bridge), reflecting the expected strain distribution. This method ensures that only relevant peaks, corresponding to structural responses rather than noise, are detected. Furthermore, as depicted in Figure 12, these peaks persist throughout the monitoring period when the truck is stationary, confirming their consistency rather than indicating transient anomalies. They likely indicate concrete cracks or stress concentrations, which, for this case study, cannot be confirmed through visual inspection or unmanned aerial vehicle (UAV) photogrammetry due to the protective steel plates covering the fiber optic locations. Since the available data do not allow differentiation between cracks and stress concentrations, all strain peaks are conservatively treated as cracks. The relative crack opening (positive strain) and relative crack closing (negative strain) are evaluated by integrating the strain over the effective influence length of the crack.

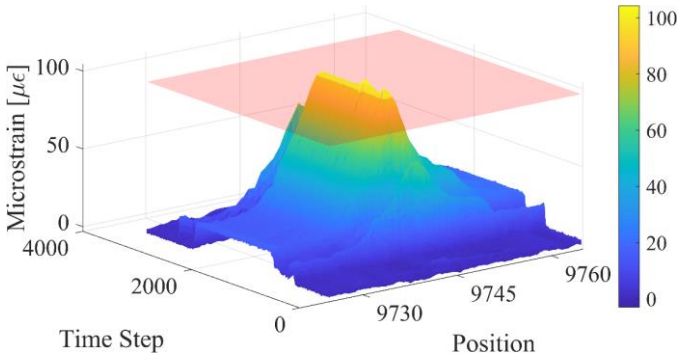

Figure 12. Consistency of DFOS measurements at peak A location in time.

Figure 13 presents histograms of relative crack opening and closing, clearly showing that the magnitudes are very low and do not pose structural concerns. The term ‘relative’ is used because the DFOS signal captures only the strain induced by the load test, not pre-existing crack widths. The width of pre-existing cracks and the causes of these strain peaks will be investigated in future monitoring campaigns. Additionally, some data are absent on the right side of the signal, but given the high spatial resolution (2.6 mm gauge pitch), the dataset remains sufficiently consistent for analysis.

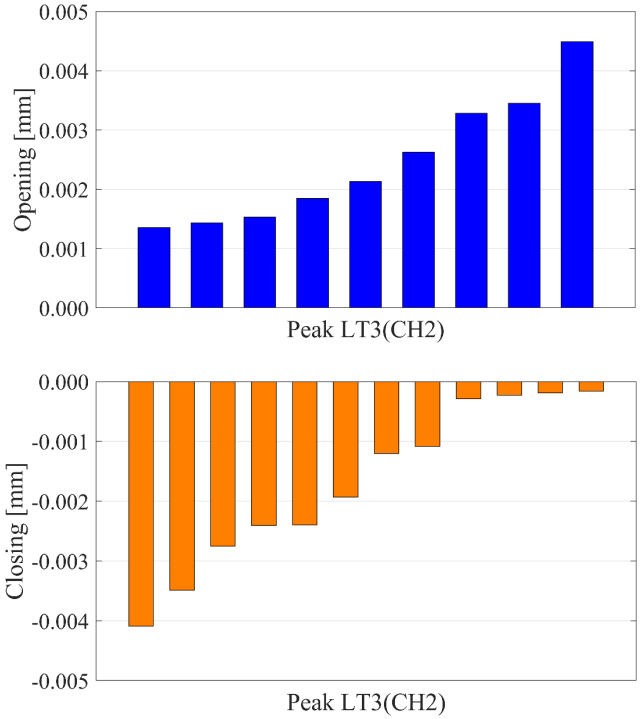

Figure 13: Crack width variation for LT3 in CH2. (Up) Relative crack opening; (Down) Relative crack closing.

The analysis of DFOS data highlights the localized impacts on strain distribution at the interfaces between the main girders and secondary beams, significantly shaped by the specific load configurations applied. The strain distribution across CH1 and CH2 displays distinct localized effects near the crossbeam edges. The LT3 load configuration induces a noticeable strain

DOI: 10.3217/978-3-99161-057-1-022

reduction near the junctions with secondary beams, as evident in Figure 14.

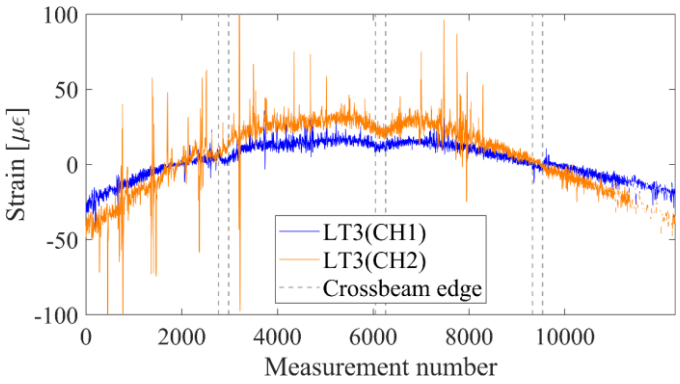

Figure 14. Strain measurements along the main girders for LT3 data of 2024.

This phenomenon stems from the transverse positioning of the axial load and the three-dimensional interactions between the main girders and secondary beams.
At this stage, the structural performance can be assessed using three key parameters:

- transverse load distribution between the main girder, quantifying the traffic load carried by each girder;
- boundary conditions;
- deflection of the main girders.

The transverse load distribution is evaluated by analyzing the strain ratio from DFOS datasets for the two main girders. This approach captures the influence of structural characteristics and load configurations while ensuring robustness by minimizing the impact of localized anomalies through reliance on spatially continuous strain data.
To illustrate the effectiveness of DFOS measurements, five monitoring scenarios are examined, each using different methods to calculate load distribution coefficients derived from sensor data:

- Scenario 1 uses strain data from the DFOS, focusing on the ratio between CH1 and CH2 measurements;
- Scenario 2 employs values calculated from equilibrium equations based on classical beam theory (De Saint-Venant), typically used in bridge assessments without monitoring data;
- Scenario 3 relies on discrete strain measurements at midspan, simulating a conventional strain gauge at that location;
- Scenario 4 combines discrete strain measurements at midspan and quarter-span strain data;
- Scenario 5 integrates discrete strain measurements at midspan and near-support measurements.

Results for load distribution coefficients ($\epsilon_{CH2}/\epsilon_{CH1}$) for LT3 are presented in Figure 15. The strain ratios using DFOS display a near-Gaussian distribution. For Scenario 1, the strain ratio is thus taken as the mean value of this distribution. When calculated using only discrete measurements (Scenarios 3 to 5), the results are substantially affected by local phenomena linked to boundary effects and strain variability at critical sections. Moreover, employing classical pre-design approaches based on equilibrium equations (Scenario 2), the strain ratio obtained differs significantly from the measured DFOS strain ratio, indicating that load distribution between girders is more balanced than suggested by conservative design assumptions.

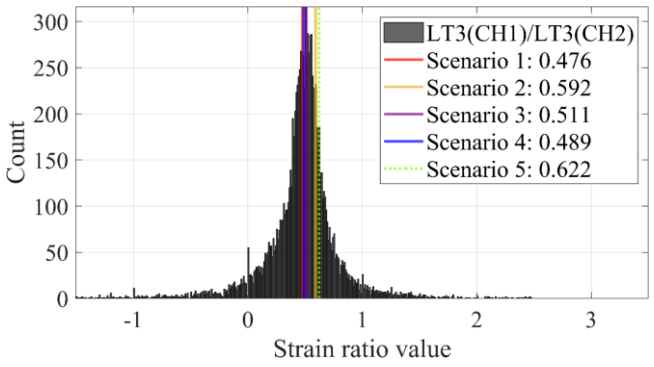

Figure 15. Transversal load distribution evaluation.

These scenarios result in inaccurate bending moment evaluations, as shown in Figure 16, potentially overestimating or underestimating safety.

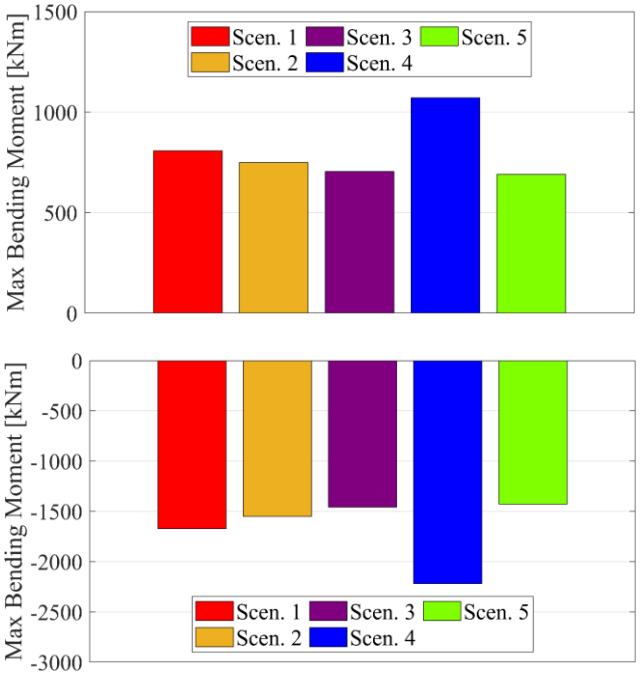

Figure 16. Bending moment comparison. (Up) Maximum bending moment in CH2; (Down) Minimum bending moment in CH2.

Once the load distribution is established, the characterization of boundary conditions becomes essential. These are evaluated by comparing DFOS strain profiles with theoretical distributions for simply supported and fixed-fixed configurations (Figure 17). From the graph, the theoretical fixed-fixed model closely aligns with the observed data (negative strains at supports, positive at midspan), confirming the post-intervention static scheme. Minor discrepancies, due to uncertainties in elastic modulus (E), stiffnesses of abutments, and load distribution coefficients, do not compromise this conclusion, confirming the structural modification's effectiveness.

DOI: 10.3217/978-3-99161-057-1-022

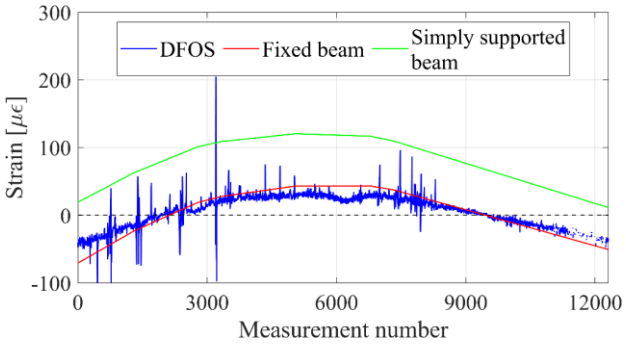

Figure 17. Boundary-condition valuation in CH2 under LT3.

Subsequently, bridge deflection is derived from DFOS datasets via double integration of the strain profile, following the methodology outlined in [8]. This process relies on load distribution data, boundary conditions, and structural rigidity. Since the latter cannot be directly measured from DFOS datasets, it is approximated between 33 GPa (C30/37) and 42 GPa (C80/95). Simulations with different rigidity values enable defining an envelope of possible bridge deflections, with the best fit, calibrated across all five load tests, determined by aligning rigidity with LVDT measurements, as shown in Figure 18.

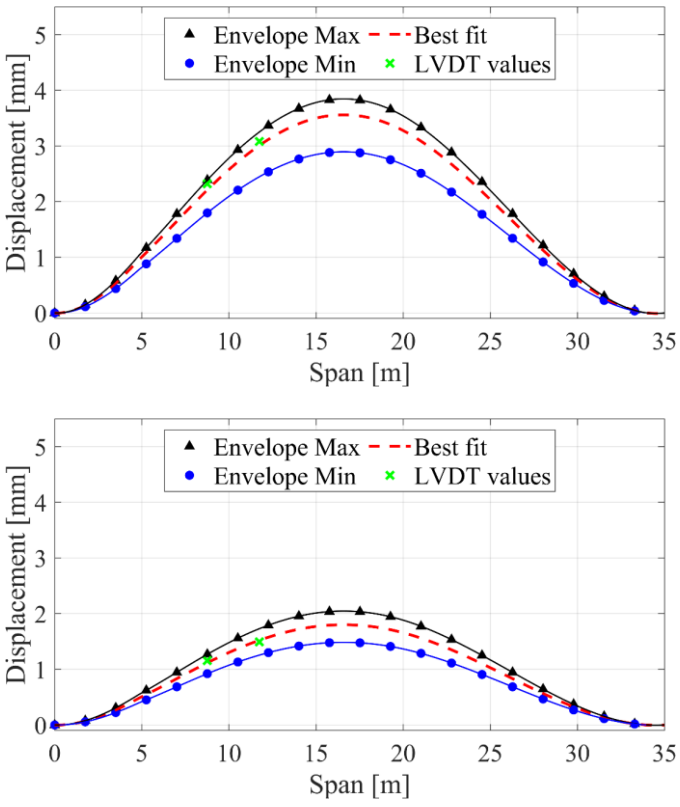

Figure 18. Comparison DFOS displacement predictions vs LVDT measurements under LT3. (Up) Comparison in CH2; (Down) Comparison in CH1.

The mean discrepancy between best-fit predictions and LVDT measurements, considering all load tests (LT1 to LT5) for both channels (CH1 and CH2), is 0.065 mm. This compares favorably to the 0.101 mm mean absolute difference reported in [8] using 2023 datasets, possibly due to greater uncertainty in LVDT positioning in 2023 compared to 2024. The small differences between these predictions demonstrate that DFOS-based deflection estimates can closely match actual measurements when rigidity is calibrated.

Furthermore, the impact of discrete strain measurements and conservative pre-design assumptions on displacement prediction is evaluated. Table 1 presents the maximum, minimum and mean absolute relative displacement differences between DFOS and LVDT measurements for Scenarios 1 to 5. The maximum difference increases significantly from Scenario 1 (0.162 mm) to others: 405% (0.818 mm) in Scenario 2, 253% (0.571 mm) in Scenario 3, 1909% (3.252 mm) in Scenario 4, and 264% (0.590 mm) in Scenario 5. The minimum difference varies slightly, from 0.00018 mm in Scenario 4 to 0.020 mm in Scenario 3. The mean difference rises by 362% (0.299 mm) in Scenario 2, 267% (0.238 mm) in Scenario 3, 1141% (0.803 mm) in Scenario 4, and 183% (0.183 mm) in Scenario 5 relative to Scenario 1 (0.065 mm).

Table 1. Maximum, minimum, and mean absolute relative displacement values between DFOS and LVDT measurements for Scenarios 1 to 5.

	Max discrepancy [mm]	Min discrepancy [mm]	Mean discrepancy [mm]
Scenario 1	0.162	0.013	0.065
Scenario 2	0.818	0.002	0.299
Scenario 3	0.571	0.020	0.238
Scenario 4	3.252	0.0018	0.803
Scenario 5	0.590	0.005	0.183

These findings indicate that Scenarios 2 to 5 yield mean displacement estimation errors ranging from 0.2 mm to 0.8 mm, whereas Scenario 1 has a mean error around 0.065 mm, establishing it as a reliable tool for displacement monitoring. It demonstrates that load-distribution estimations using only discrete strain measurement may be inaccurate and lead to significant discrepancies in the expected bridge deflection.

4 CONCLUSIONS

This study investigates the DFOS-based methodology from [8], originally developed for 2023 datasets, to analyze the 2024 Ferpècle Bridge datasets. By evaluating strain data across both channels under various static load configurations, the approach demonstrates its ability to capture local phenomena (e.g., cracks, secondary beam effects) and global responses (e.g., boundary conditions, load distribution, displacement estimates) with exceptional accuracy and precision. Compared to traditional discrete strain sensors, DFOS offers significant advantages, yielding the following insights:

- High-resolution monitoring. DFOS enables spatially continuous strain measurements with millimeter-scale precision, accurately determining load distribution coefficients, bending moment diagrams, and displacement estimates with ~0.1 mm accuracy, surpassing the capabilities of discrete sensors.

DOI: 10.3217/978-3-99161-057-1-022

- Longitudinal (1D) crack detection. The methodology reliably identifies cracks and stress concentrations but faces challenges in classification due to limited data on pre-existing micro-crack distributions (sometimes difficult to detect due to their size and locations) and its linear sensing configuration, which restricts bi-dimensional (2D) strain mapping.
- Consistency across years. The 2024 results align closely with 2023 findings, confirming the methodology's reliability, high accuracy, and precision, while indicating no significant structural changes in the bridge.
- Future directions. Further research should investigate temperature effects under ambient daily and seasonal loads, integrate visual inspection or UAV photogrammetry alongside 2D strain mapping to enable proper crack characterization and develop a calibrated finite element model (FEM) to support long-term SHM.

This high-resolution DFOS methodology provides detailed insights into structural behavior, enabling precise safety assessments and informed decision-making for sustainable bridge maintenance and management.

ACKNOWLEDGMENTS

The authors are thankful to the Structural Engineering Platform (GIS) from École Polytechnique Fédérale de Lausanne (EPFL) and Prof. Eugen Brühwiler for supporting the data collection process. The authors are also thankful to the DMTE – Service de la mobilité from the Wallis Canton for supporting the monitoring campaign.

REFERENCES

[1] N. Bertola and E. Brühwiler, 'Risk-based methodology to assess bridge condition based on visual inspection', Structure and Infrastructure Engineering, vol. 19, no. 4, pp. 575-588, 2021. DOI: 10.1080/15732479.2021.1959621.
[2] N. Bertola et al., 'A global framework for data-informed bridge examination', Structure and Infrastructure Engineering, pp. 1–20, 2024. DOI: 10.1080/15732479.2024.2337088.
[3] M. Q. Feng et al., 'Baseline Models for Bridge Performance Monitoring', Journal of Engineering Mechanics, vol. 130, no. 5, pp. 562–569, 2004. DOI: 10.1061/(ASCE)0733-9399(2004)130:5(562).
[4] B. Glisic, 'Concise historic overview of strain sensors used in the monitoring of civil structures: The first one hundred years', Sensors, vol. 22, no. 6, pp. 2397, 2022. DOI: 10.3390/s22062397.
[5] H.-N. Li et al., 'Recent applications of fiber optic sensors to health monitoring in civil engineering', Engineering Structures, vol. 26, no. 11, pp. 1647–1657, 2004. DOI: 10.1016/j.engstruct.2004.05.018.
[6] F. I. H. Sakiyama et al., 'Structural health monitoring of concrete structures using fibre-optic-based sensors: a review', Magazine of Concrete Research, vol. 73, no. 4, pp. 174–194, 2021. DOI: 10.1680/jmacr.19.00185.
[7] L. Zhang et al., 'Over 25-year monitoring of the Tsing Ma suspension bridge in Hong Kong', J Civil Struct Health Monit, vol. 15, pp. 263–283, 2024. DOI: 10.1007/s13349-024-00842-5.
[8] F. Fabbricatore and N. Bertola, 'Methodology for concrete girder bridge performance monitoring through distributed fiber optic sensors', Structural Health Monitoring, under review, 2025.
[9] N. Bertola and E. Brühwiler, 'Transforming The Static System of Prestressed Concrete Bridges Using UHPFRC', Journal of Bridge Engineering, vol. 30, no. 7, 2025. DOI: 10.1061/JBENF2.BEENG-7234.
[10] 'SIA 269 - Existing structures', 2011.
[11] 'SIA 2052 - Béton fibré ultra-performant (BFUP) - Matériaux, dimensionnement et exécution', 2016.
[12] SMARTProfile II, Smartec, 2017. https://smartec.ch/en/product/smartprofile-ii/
[13] 'ODiSI 6100 User's Guide', 2020. https://lunainc.com/sites/default/files/assets/files/resource-library/ODiSI%206100%20User%20Guide.pdf
[14] B. Richter et al., 'Crack monitoring on concrete structures with distributed fiber optic sensors—Toward automated data evaluation and assessment', Structural Concrete, vol. 25, no. 2, pp. 1465-1480, 2023. DOI: 10.1002/suco.202300100.